Analyst

ROYAL SOCIETY OF CHEMISTRY

PAPER

View Article Online
View Journal | View Issue

Cite this: *Analyst*, 2025, **150**, 2702

The effects of different plasticisers on the electrochemical performance of bespoke conductive additive manufacturing filaments using recycled PLA†

Robert D. Crapnell, [a] Iana V. S. Arantes, [a,b] Elena Bernalte, [a] Evelyn Sigley,[a] Graham C. Smith, [c] Thiago R. L. C. Paixão [b] and Craig E. Banks *[a]

In this work, we report the production, physicochemical, electrochemical, and electroanalytical characterisation of 10 different bespoke additive manufacturing filaments that utilise different chemicals as plasticisers. The inclusion of a plasticiser within a recycled poly(lactic acid) based additive manufacturing filament produced through thermal mixing is required when incorporating high loadings of conductive fillers. All 10 chemicals used in this work acted as suitable plasticisers for producing conductive filaments, allowing the incorporation of 25 wt% carbon black with 65 wt% recycled poly(lactic acid) whilst ensuring excellent low-temperature flexibility and printability. The surfaces of the additive manufactured electrodes were characterised before and after electrochemical activation, revealing a significant increase in the amount of graphitic carbon present after activation in all cases. Through electrochemical characterisation against $[Ru(NH_3)_6]^{3+}$ and $[Fe(CN)_6]^{4-}$, as well as through the electroanalytical detection of dopamine, castor oil, tris(2-ethylhexyl) trimellitate, and poly(ethylene glycol) were identified as the best overall performing plasticisers for the production of additively manufactured electrodes.

Received 10th July 2024,
Accepted 29th April 2025

DOI: 10.1039/d4an00969j

rsc.li/analyst

1. Introduction

Additive manufacturing (3D-printing) is the general name for a group of manufacturing methodologies in which a computer-aided design (CAD) file is processed into physical objects through the deposition of materials in a layer-by-layer fashion. In general, additive manufacturing and 3D-printing are blanket terms applied to at least seven different manufacturing methodologies, outlined in "ASTM F42 – Additive Manufacturing".[1] In the field of electrochemistry, Fused Filament Fabrication (FFF, also known as Fused Deposition Modelling or FDM) has seen a rapid rise in use within the scientific community. This is due in part to its inexpensive entry level and reproducible results, with robust and reliable printers available for less than £500 and conductive commercial filaments available for only approximately one hundred pounds per kg.[2]

In the electrochemical scientific literature, the majority of works are published using commercially available conductive filaments, of which two are commonly used and have been in use for many years with minimal competitors. Using such filaments, researchers have produced additively manufactured platforms in various areas of electrochemistry, including energy storage devices,[3,4] electrochemical water splitting,[5,6] electroanalysis in forensics[7,8] and environmentally interesting chemicals,[9,10] and for the production of electrochemical biosensing devices.[11–14] Although these reports show their successful applications, their performance is generally substandard compared to those of other electrode materials, and is down to the performance of the filament. As such, there have been numerous studies looking at ways to improve the performance of electrodes produced from these commercial conductive filaments, such as "activating" through the removal of surface PLA,[15] changing the electrode shape,[16] altering the printing temperature[17] or speed,[18,19] electroplating[20] and shortening the connection length.[21] Even with all of these improvement methods, the final performance of electrochemical platforms using commercial filaments lacks sufficient quality. The production of new, high-performance, bespoke conductive filaments is required for

[a]*Faculty of Science and Engineering, Manchester Metropolitan University, Chester Street, Dalton Building, Manchester, M1 5GD, Great Britain. E-mail: c.banks@mmu.ac.uk; Tel: +44(0)1612471196*
[b]*Departamento de Química Fundamental, Instituto de Química, Universidade de São Paulo, São Paulo, SP, 05508-000, Brazil*
[c]*School of Natural Sciences, Faculty of Science, Business and Enterprise, University of Chester, Parkgate Road, Chester CH1 4BJ, UK*
† Electronic supplementary information (ESI) available. See DOI: https://doi.org/10.1039/d4an00969j

additive manufacturing electrochemistry to realise its full potential.

There has been a rise in reports in recent years on bespoke conductive filaments for FFF additive manufacturing, which mainly focus on two different methodologies for production: solvent mixing and thermal mixing.[22] Solvent mixing is a cheaper option for entry into this field, whereby the bulk polymer is dissolved in a solvent matrix, and then stirred with the desired amount of conductive material. The solvent is then removed, leaving the conductive composite ready for granulation and transforming into a filament. Overall, simple and easily accessible, solvent-based methods suffer from long preparation times as a consequence of the long dissolution and evaporation/drying steps.[22] Contrastingly, thermal mixing involves heating the polymeric matrix in a sealed chamber, while simultaneously incorporating the conductive filler through mixing blades. This process is significantly quicker than the solvent method, improves the dispersion of the nanomaterials, and is considered more environmentally friendly due to the lack of the requirement of potentially hazardous solvents. However, this methodology has a significantly increased start-up cost, with the requirement of sophisticated and costly equipment and infrastructure.[22]

One additional requirement for producing high filler loadings within a poly(lactic acid) (PLA) filament using the thermal mixing method is the incorporation of a plasticiser. The plasticiser is defined by The Council of the International Union of Pure and Applied Chemistry (IUPAC) as follows: "A plasticiser is a substance or material incorporated in a material (usually plastic or elastomer) to increase its flexibility, workability, or distensibility",[23] and is absolutely vital for creating a filament that has low-temperature flexibility required for reproducible and high-performance printing. In the published literature on bespoke conductive additive manufacturing filaments there have been numerous different plasticisers reported. One of the first plasticisers used was poly(ethylene glycol) (PEG), where Ghosh and co-workers[24] included 18.2 wt% in a filament with activated charcoal and MoS_2 that showed good (photo)electrocatalytic properties. Additionally, Wuamprakhon and co-workers[25] also used PEG at a loading of 10 v/v% alongside carbon black to produce additively manufactured aqueous supercapacitors. In both these works, the charge storage capabilities of the filaments were highlighted. In contrast, Sigley and co-workers[26] developed a filament for use in electroanalysis by incorporating poly(ethylene succinate) (PES) at 8.78 wt% with carbon black, which gave a stable and low background current. Due to the relatively high cost of PES, Arantes and co-workers[27] utilised tris(2-ethylhexyl) trimellitate (TOTM) at 10 wt% to produce a high-performance filament for use in a portable electrochemical sensing platform for beverage adulterants. Although all of these filaments show good performance, Crapnell and co-workers[28] changed the plasticiser to a bio-based product, castor oil, showing that this produced a filament with excellent conductivity and low-temperature flexibility. This method of using castor oil along with recycled PLA to improve the sustainability of the bespoke filaments has been used in further work for electroanalytical applications,[29,30] highlighting the reliability of this combination.

It is clear, especially when comparing poly(ethylene glycol) to other compounds, that the plasticiser used in the production of bespoke conductive additive manufacturing filaments has a significant impact on the performance. As such, in this work we look to produce 10 filaments with different plasticisers, all with identical loadings of carbon black into the same supply of recycled PLA. Through physicochemical and electrochemical characterisation of the electrodes printed from these filaments, we aim to show the effect that the plasticiser can have and help guide researchers toward options for their own filament production.

2. Experimental section

2.1 Chemicals

All chemicals used were of analytical grade and were used as received without any further purification. All solutions were prepared with deionised water with resistivity not less than 18.2 MΩ cm from a Milli-Q Integral 3 system from Millipore UK (Watford, UK). Hexaaminеruthenium(III) chloride (98%), potassium ferricyanide(III) (99%), potassium hexacyanoferrate (II) trihydrate (98.5–102.0%), sodium hydroxide (>98%), potassium chloride (99.0–100.5%), dopamine hydrochloride (≥99%), castor oil (CO), dioctyl terephthalate (DOTP, ≥96%), tributyl citrate (TBC, ≥97%), bis(2-ethylhexyl) adipate (DEHA, ≥97%), poly(ethylene succinate) (PES, MW = 10 000), poly(ethylene glycol) (PEG, MW = 3000) and phosphate-buffered saline (PBS) tablets were purchased from Merck (Gillingham, UK). Carbon black (CB Super P®, >99+%) was purchased from Fisher Scientific (Loughborough, UK). Tris(2-ethylhexyl) trimellitate (TOTM, >97%), diethylene glycol dibenzoate (DEGDB, >97%), diisodecyl phthalate (DIDP), and diisononyl phthalate (DINP) were purchased from TCI chemicals (Oxford, UK). Recycled poly(lactic acid) (rPLA) was purchased from Gianeco (Turin, Italy). A commercial conductive PLA/carbon black filament (1.75 mm, Protopasta, Vancouver, Canada) was purchased from Farnell (Leeds, UK).

2.2 Recycled filament production and additive manufacturing

Recycled filaments were processed using a Thermo Haake Polydrive dynameter fitted with a Thermo Haake Rheomix 600 (Thermo-Haake, Germany), a Rapid Granulator 1528 (Rapid, Sweden) and an EX6 extrusion line (Filabot, VA, United States) producing a 1.75 mm diameter of filament. All computer designs and .3MF files seen throughout this manuscript were produced using Fusion 360® (Autodesk®, CA, United States) and are sliced and converted to .GCODE files ready for printing by the printer specific software, PrusaSlicer (Prusa Research, Prague, Czech Republic). The additively manufactured electrodes were 3D-printed using fused filament fabrication (FFF) technology on a Prusa i3 MK3S+ (Prusa Research, Prague, Czech Republic) using a 0.6 mm nozzle with a nozzle

temperature of 215 °C, 100% rectilinear infill, 0.15 mm layer height, and a print speed of 70 mm s^{-1}.

2.3 Physicochemical and electrochemical characterisation

X-ray Photoelectron Spectroscopy (XPS) data were acquired using an AXIS Supra (Kratos, UK), equipped with a monochromated Al X-ray source (1486.6 eV) operating at 225 W and a hemispherical sector analyser. Scanning Electron Microscopy (SEM) measurements were performed on a Supra 40VP Field Emission (Carl Zeiss Ltd, Cambridge, UK) with an average chamber and gun vacuum of 1.3×10^{-5} and 1×10^{-9} mbar, respectively. All electrochemical measurements were performed on an Autolab 100N potentiostat controlled by NOVA 2.1.6 (Utrecht, the Netherlands). The electrochemical characterisation of the bespoke filament and comparison to the benchmarks were performed using lollipop design (∅ 5 mm, 18 mm connection length, and 1 mm thickness) electrodes alongside an external commercial Ag|AgCl (3 M KCl) reference electrode and a nichrome wire counter electrode. Activation of the additive manufactured electrodes was achieved through chronoamperometry within an aqueous sodium hydroxide solution (0.5 M) and applying +1.4 V for 200 s, followed immediately by applying −1.0 V for 200 s. After this, the additive manufactured electrodes were removed from the solution, rinsed with deionised water and dried under a stream of nitrogen. Further details are included in the ESI† section.

3. Results and discussion

3.1 Production and characterisation of recycled filaments

In this work, 10 different bespoke conductive filaments were produced in identical ways to that previously reported in the literature.[26–28] Briefly, the materials were all placed within the heated chamber (190 °C) of a Thermo Haake Rheomix 600, and mixed with Banbury rotors at 70 rpm for 5 min. Once mixed, the polymer composites were recovered, cooled, and shredded to produce particulates small enough for extrusion. These particles were then fed into the hopper of a Filabot EX6, where they were extruded into 1.75 mm diameter filaments ready for use on a FFF 3D-printer. All filaments utilised identical sources and weights of recycled PLA polymer (65 wt%) and carbon black (25 wt%) feedstocks, but each was prepared using 10 wt% of different chemicals acting as the plasticiser. The plasticisers explored throughout this work are dioctyl terephthalate (DOTP), diisononyl phthalate (DINP), diisodecyl phthalate (DIDP), poly(ethylene glycol) (PEG), poly(ethylene succinate) (PES), tributyl citrate (TBC), castor oil (CO), bis(2-ethylhexyl) adipate (DEHA), diethylene glycol dibenzoate (DEGDB), and tris(2-ethylhexyl) trimellitate (TOTM), and their chemical structures can be found in Scheme 1. We note that PEG,[24,25] PES,[26,31] CO[28–30] and TOTM[27] have been reported previously toward the production of conductive filaments for electrochemical applications but find their inclusion and collation of data into a single study to be extremely useful for researchers in this field.

In the case of all the plasticisers, reproducible and conductive filaments were produced with excellent low-temperature flexibility. Without the addition of any chemicals, the maximum amount of carbon black that could be incorporated into the PLA was ~17 wt%, highlighting the ability of all of these chemicals to act as a suitable plasticiser for the production of conductive filaments. The 10 different bespoke filaments were all printed using an identical printing file and identical printing parameters before use in electrochemical experiments. In the field of electrochemistry, it is a routine task to "activate" additively manufactured electrodes after printing and before use to improve their electrochemical performance toward inner-sphere probes.[15,18] In this work, we utilised the most commonly found activation method for additive manufactured electrodes which is through the application of chronoamperometry in an aqueous solution of sodium hydroxide (0.5 M).[32] Fig. 1 shows the scanning electron micrographs obtained for additively manufactured electrodes printed from all 10 filaments before (top left) and after (bottom right) this activation procedure. In all cases, it can be seen that the surface of the additively manufactured electrode is predominantly covered by a smooth layer of the PLA, which is effectively stripped from the surface through the activation procedure to reveal the carbon black embedded beneath.

This is further supported through X-ray photoelectron spectroscopy data found in Fig. 2 and Table S1,† where it can be seen that for all electrodes, there is a large increase in the atomic percentage (at%) found for the graphitic carbon peak in the activated sample. Fig. 2 shows an example of this significant change for both DIDP and TBC plasticisers. DIDP produced the most significant increase in the graphitic carbon peak upon activation, going from 0% with the freshly printed additively manufactured electrodes, Fig. 2A, to 52% after the activation, Fig. 2B. This suggests that there is no carbon black present on the surface of the additively manufactured electrode after the printing, but the electrochemical activation removes a large amount of surface polymer and plasticiser. In contrast, an asymmetric peak was required for adequate fitting of even the non-activated additively manufactured electrodes printed with TBC as the plasticiser, indicating a small amount of surface carbon black. The difference between the hydrocarbon-like and graphite C 1s components appears quite large, but it is consistent with recent reviews,[33–35] particularly when the possible effect of differential electrostatic charging between the substrate and the surface layers is taken into account.[36]

The XPS C 1s spectrum for the DIDP as-printed electrode, Fig. 2A, differs significantly from the XPS spectrum obtained for solely PLA, which comprises three peaks of similar intensity, corresponding to equal amounts of three carbon environments present within the PLA backbone.[26] In the case of the C 1s environment for DIDP the peak at 285.0 eV, denoted as the C–C bonding peak, had a significantly larger magnitude than the C–O or O–C=O peaks, which is expected to be due to the large CH_2 side chains of the structure, seen in Scheme 1. This

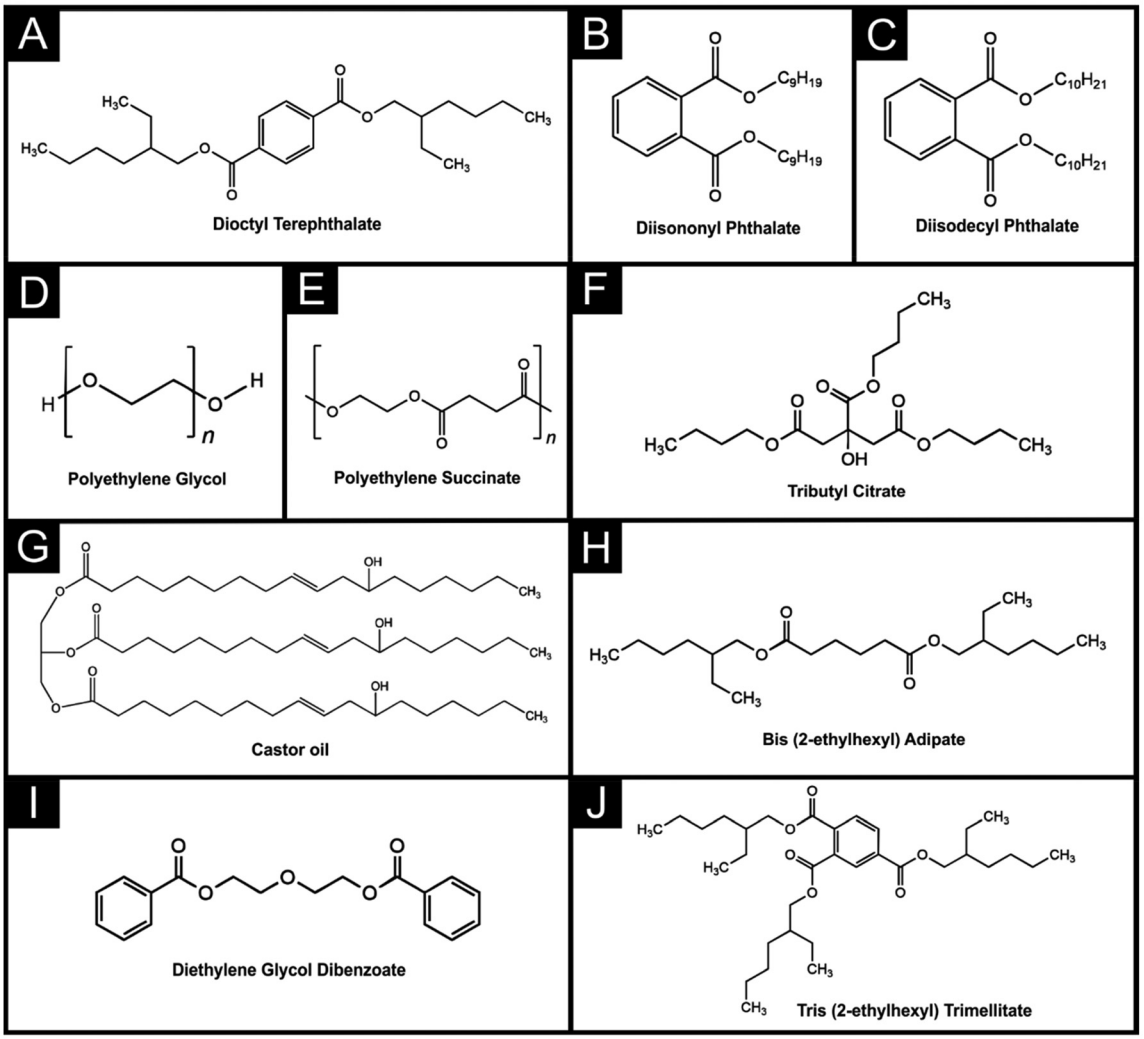

Scheme 1 Chemical structures for the different chemicals used as plasticisers throughout this work. (A) Dioctyl terephthalate; (B) diisononyl phthalate; (C) diisodecyl phthalate; (D) poly(ethylene glycol); (E) poly(ethylene succinate); (F) tributyl citrate; (G) castor oil; (H) bis(2-ethylhexyl) adipate; (I) diethylene glycol dibenzoate; and (J) tris(2-ethylhexyl) trimellitate.

indicates that a significant amount of the plasticiser is present on the surface of the printed additively manufactured electrodes. In contrast, the as-printed spectra obtained for TBC, Fig. 2C, is much more similar to that of PLA, which is consistent with the structure seen in Scheme 1. This phenomenon can be seen in the case of all as-printed additively manufactured electrodes, Fig. S1,† where the C 1s spectra vary significantly, but all relate back to the chemical structure of the plasticiser seen in Scheme 1. All corresponding O 1s spectra can be seen in Fig. S2.† The C–C/C–H components are charge referenced to 284.8 eV and those of all the O–C=O components are in agreement within a fraction of an eV. Upon activation, Fig. 2B, the introduction of a new asymmetric peak is required at 284.5 eV for adequate fitting, which is attributed to the X-ray photoelectron emission by graphitic carbon.[37,38] This matches what is seen in the SEM images in Fig. 1C, indicating that the removal of the surface polymeric and plasticiser material has indeed revealed significant amounts of carbon black. Similarly, in Fig. 2D, a much larger graphitic carbon peak is obtained for the activated TBC additively manufactured electrode, indicating the presence of significantly larger amounts of graphitic carbon. Once again, the same phenomenon is seen for the other 8 electrodes in Fig. S3.† All corresponding O 1s spectra can be seen in Fig. S4.† A summary of the atomic percentages found within the C 1s environment before and after activation for additively manufactured electrodes printed from each of the 10 filaments is presented in Table S1,† where similar trends in the increase of the required graphitic carbon peak can be found.

3.2 Electrochemical characterisation of additively manufactured electrodes

The as-printed additively manufactured electrodes were initially tested electrochemically against the near-ideal outer-sphere redox probe hexaammineruthenium(III) chloride ([Ru

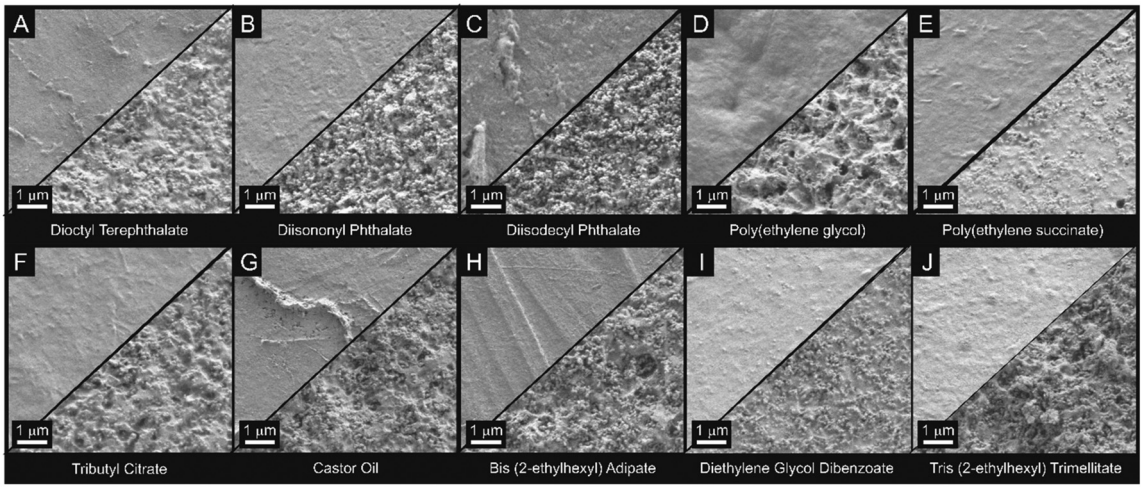

Fig. 1 SEM images corresponding to the as-printed (top left) and activated (bottom right) printed additively manufactured electrodes utilising different plasticisers. (A) Dioctyl terephthalate (DOTP); (B) diisononyl phthalate (DINP); (C) diisodecyl phthalate (DIDP); (D) poly(ethylene glycol) (PEG); (E) poly(ethylene succinate) (PES); (F) tributyl citrate (TBC); (G) castor oil (CO); (H) bis(2-ethylhexyl) adipate (DEHA); (I) diethylene glycol dibenzoate (DEGDB); and (J) tris(2-ethylhexyl) trimellitate (TOTM).

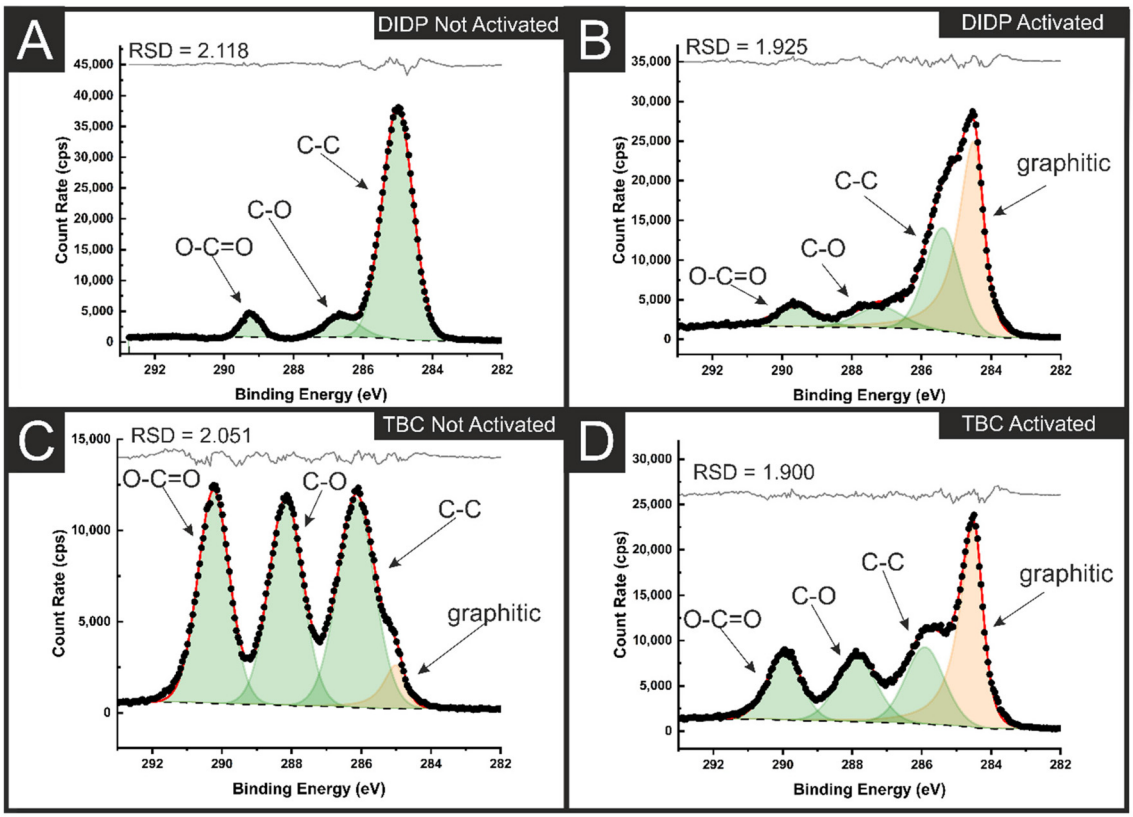

Fig. 2 XPS C 1 S spectra for (A) non-activated and (B) activated electrodes with DIDP as a plasticiser. XPS C 1 S spectra for (C) non-activated and (D) activated electrodes with TBC as a plasticiser.

$(NH_3)_6]^{3+}$, 1 mM in 0.1 M KCl) through cyclic voltammetric scan rate studies (5–500 mV s^{-1}). Examples of these scan rate studies for additively manufactured electrodes with DEHA and PEG as the plasticisers are presented in Fig. 3A and B, with the corresponding Randles–Ševčík plot inset. In all cases, the Randles–Ševčík plots obtained showed excellent linearity, confirming the diffusion-controlled nature of the redox phenomenon. A comparison of the response toward $[Ru(NH_3)_6]^{3+}$

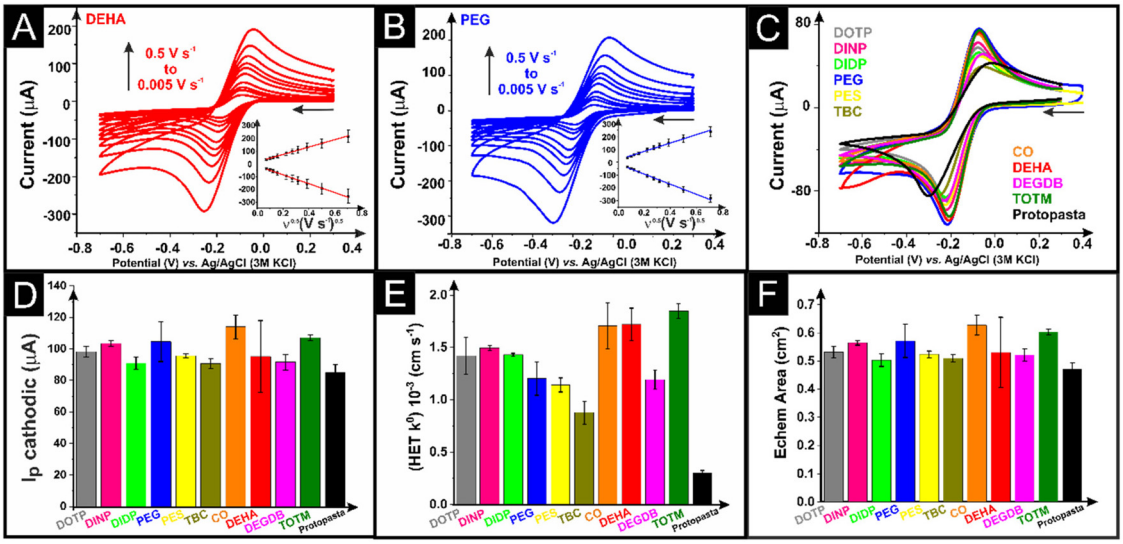

Fig. 3 Cyclic voltammograms (5–500 mV s^{-1}) of $[Ru(NH_3)_6]^{3+}$ (1 mM in 0.1 M KCl) with (A) CB/PLA/DEHA and (B) CB/PLA/PEG as the WE, nichrome coil as the CE, and Ag|AgCl as the RE. The Randles–Ševčík plots are presented in the inset. (C) Comparison of the $[Ru(NH_3)_6]^{3+}$ cyclic voltammograms (50 mV s^{-1}) for the bespoke CB/PLA filaments made with different plasticisers and the commercial CB/PLA filament (Protopasta). (D) Cathodic peak currents (I_{pc}) extracted from the $[Ru(NH_3)_6]^{3+}$ cyclic voltammograms (50 mV s^{-1}) and the respective (E) heterogeneous electron transfer rate constant (HET k^0) values and the (F) electrochemical areas calculated using the Randles–Ševčík equation with full scan rate studies for all bespoke filaments.

(1 mM in 0.1 M KCl) for additively manufactured electrodes printed from all 10 different bespoke compositions, alongside the most commonly used commercial filament, is presented in Fig. 3C. It can be seen that every bespoke filament offers a significant improvement in the electrochemical response of $[Ru(NH_3)_6]^{3+}$, both in terms of the peak currents obtained and the peak-to-peak separations (ΔE_p) (Fig. S5A†). In terms of the peak cathodic current, the average recorded value at a scan rate of 50 mV s^{-1} (n = 3) for each filament is summarised in Fig. 3D, showing that all bespoke filaments produce larger peak currents when compared to the commercial example, with the CO and TOTM plasticisers showing excellent performance. This shows that any of these chemicals can be successfully utilised as a plasticiser to make high-quality conductive filaments for electrochemical experiments. We note, however, that this work focuses on testing the additive manufactured electrodes made from filaments with 25 wt% loading of carbon black and does not test the maximum loadings of carbon possible with each plasticiser as this may vary significantly.

The scan rate study data were utilised to calculate the heterogeneous electron transfer rate constant (k^0) and the electrochemically active area of the electrodes (A_e),[39] where the averages (n = 3) are presented in Fig. 3E and F, respectively. The calculated k^0 data in Fig. 3E clearly show significant variation in the performance of the additively manufactured electrodes using different plasticisers. It is important to first note how all of the bespoke filaments considerably outperform the commercial example. In Fig. 3F, there is less variation in A_e, with the value of the commercial example being the lowest as expected due to the slightly lower carbon loading. The best-performing additively manufactured electrodes in this instance for k^0 were CO, DEHA and TOTM, although the DEHA additively manufactured electrodes presented a much larger standard deviation in terms of their peak currents and A_e values. It is particularly interesting that the CO additively manufactured electrode performs so well, and the XPS data show no presence of any graphitic carbon on the surface of the electrode, highlighting how the outer-sphere redox probe $[Ru(NH_3)_6]^{3+}$ does not need direct access to the carbon surface for the electrochemical redox reaction to occur. This is why electrochemical activation is so commonly used in the field of additive manufacturing electrochemistry, as inner-sphere redox reactions cannot take place within such a system.[18] As such, it is important to characterise the additively manufactured electrodes after identical activations against an inner-sphere redox probe such as $[Fe(CN)_6]^{4-}$ (1 mM in 0.1 M KCl). Examples of scan rate studies (5–500 mV s^{-1}) for this using CO and PEG additively manufactured electrodes are presented in Fig. 4A and B, respectively, with a comparison of all bespoke additively manufactured electrodes and the commercial additively manufactured electrode at 50 mV s^{-1} presented in Fig. 4C. Note that our heterogeneous electron transfer rate constant (k^0) is higher than other reported values of 5.9×10^{-5} cm s^{-1} (ref. 19) and 9.5×10^{-6} cm s^{-1} both obtained with the use of ferri/ferrocyanide and ProtoPasta filaments which were modified to report a value of 9.0×10^{-3} cm s^{-1} using laser treatment.[40] It is impossible to compare different responses accurately since we used a reduced connection length in line with our previous data where we showed that the contact distance influences the cyclic voltammetric profile using a planar electrode[21] which was expanded using an in-laid disc.[40] Furthermore, our data

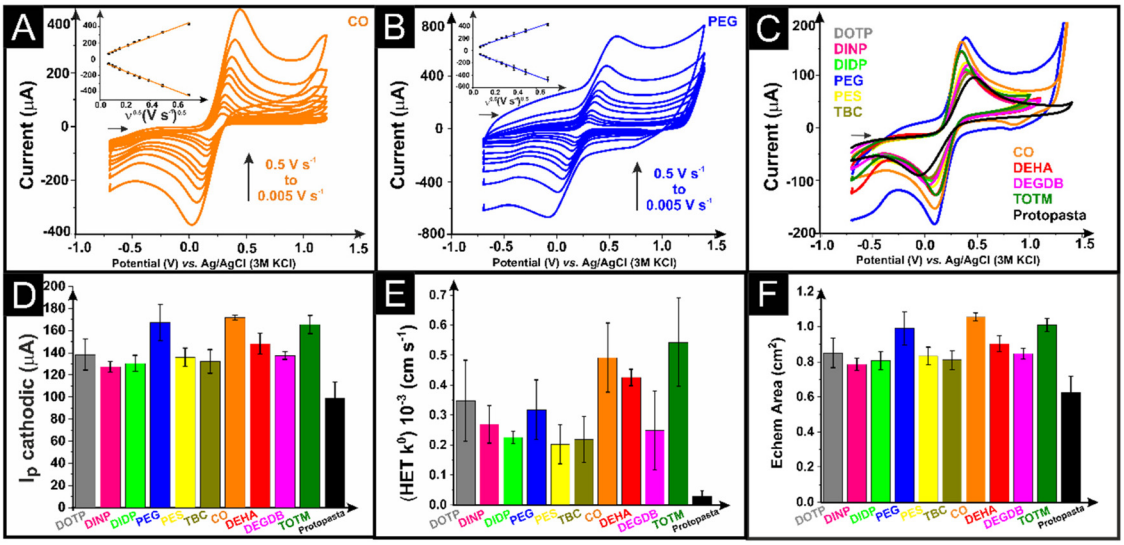

Fig. 4 (A) Cyclic voltammograms (5–500 mV s^{-1}) of ferri/ferrocyanide (1 mM in 0.1 M KCl) with (A) CB/PLA/CO and (B) CB/PLA/PEG as the WE, nichrome coil as the CE, and Ag|AgCl as the RE. The Randles–Ševčík plots are presented in the inset. (C) Comparison of the ferri/ferrocyanide cyclic voltammograms (50 mV s^{-1}) for the bespoke CB/PLA filaments made with different plasticisers and the commercial CB/PLA filament (Protopasta). (D) Cathodic peak currents (Ip_c) extracted from the ferri/ferrocyanide cyclic voltammograms (50 mV s^{-1}) and the respective (E) heterogeneous electron transfer rate constant (HET k^0) values and the (F) electrochemical areas calculated using the Randles–Ševčík equation with full scan rate studies for all bespoke filaments.

are obtained from optimised bespoke filaments that we constructed from recycled PLA polymer (65 wt%) and carbon black (25 wt%) feedstocks, but each was prepared using 10 wt% of different chemicals acting as the plasticiser. Finally, it is important to realise that the different plasticisers give rise to different surface moieties in the form of oxygenated species (see Table S1†) which will influence the inner-sphere redox profile as previously reported using basal plane and edge plane pyrolytic graphite electrodes.[41]

Once again, it is clear that all of the bespoke filaments outperform the commercial standard. Interestingly, the PEG-based additively manufactured electrodes in Fig. 4B and C show a vastly different voltammetric profile from all of the other systems, with very large background currents observed. This is due to the tendency of PEG to dissociate ion pairs into free ions, which leads to an increase in conductivity.[42] This is a prime example of why this plasticiser has been preferentially chosen in some applications toward the production of additively manufactured electrochemical supercapacitors.[24,25] Even so, it can be seen that the PEG plasticiser additively manufactured electrode is one of the best performing, alongside CO and TOTM, when taking into account the peak currents, k^0 and A_e values obtained in Fig. 4D, E and F, respectively, and the peak-to-peak separations (ΔE_p) in Fig. S5B.† Once again, these data confirm that all of the plasticisers presented in this work can produce conductive filaments suitable for electrochemical activity.

3.3 Electroanalytical application

To further test the additively manufactured electrodes produced from filaments with different plasticisers, they were applied to the electroanalytical detection of the well-known analyte dopamine through cyclic voltammetry (50 mV s^{-1}). An example of the detection of dopamine (10–500 μmol L^{-1}) using an additively manufactured electrode produced with CO as the plasticiser is presented in Fig. 5A, with examples of all other plasticisers presented in Fig. S6.†

A comparison between the 10 bespoke additively manufactured electrodes and the commercial example for the detection of dopamine (100 μmol L^{-1}) is presented in Fig. 5B, where there are substantial differences in the voltammograms obtained. It should be noted that due to the short experimental time of electroanalysis the potential leeching of the plasticiser or ingress of solution over time is not considered. The PEG-plasticised additively manufactured electrode once again exhibits a significantly larger background current compared to any of the other additively manufactured electrodes, and the CO additively manufactured electrode once again performs extremely well. Interestingly, many of the additively manufactured electrodes exhibit an anodic shift in the peak potential obtained for dopamine. This could be indicative of either a worse electrochemical performance or an increase in the adsorption of dopamine to these surfaces, as the anodisation and surface roughness have been shown to affect the dopamine adsorption efficiency.[43] In Fig. 5C, the obtained calibration plots for each additively manufactured electrode are presented, with all showing good linearity. It is important to note that the additively manufactured electrodes made from DOTP did not show a suitable voltammogram for the highest concentration of dopamine, and, therefore, even though a good sensitivity was obtained, the overall linear range is the worst. When comparing the sensitivities calculated in Fig. 5D, the PEG and CO-plasticised additively manufactured electrodes

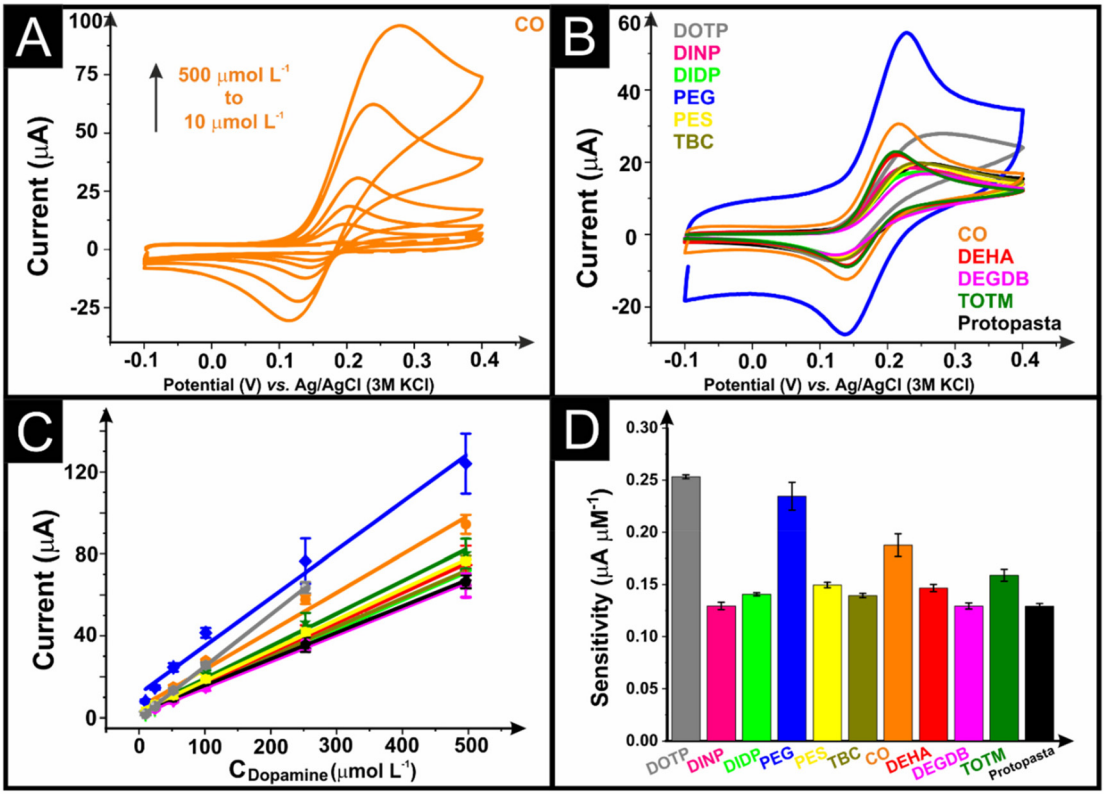

Fig. 5 (A) Cyclic voltammograms (50 mV s^{-1}) of dopamine at different concentrations (10, 25, 50, 100, 250, and 500 μM) in 0.1 M PBS pH 7.4 with CB/PLA/CO as the WE, nichrome coil as the CE, and Ag|AgCl as the RE. (B) Comparison of 100 μM dopamine CVs (50 mV s^{-1}). (C) Calibration curves for dopamine at different concentrations, and (D) bar plot for dopamine sensitivity for the bespoke CB/PLA filaments made with different plasticisers and the commercial CB/PLA filament. All data are obtained with n = 3 with the average and standard deviations presented.

stand out again as the best performing, along with the TOTM. These electrodes have consistently performed well throughout the electrochemical and electroanalytical testing, and we therefore suggest their use for the production of additive manufacturing of filaments toward these aims.[27,28] Due to the excellent conductivities and flexibilities we have obtained with all of these filaments they could be used in various other applications such as printed electronics.

4. Conclusions

This work presents the fabrication of 10 bespoke conductive filaments for the production of additively manufactured electrodes through fused filament fabrication. Each filament was manufactured using the same experimental procedure, with identical amounts of carbon black (25 wt%) and recycled poly (lactic acid) (65 wt%), but each with a different chemical included as a plasticiser at a loading of 10 wt%. Each chemical produced a conductive filament with excellent low-temperature flexibility, printability, and good conductivity. The surfaces and surface composition of the as-printed and electrochemically activated electrodes were characterised through SEM and XPS, revealing a large increase in the amount of graphitic carbon present after activation.

The additively manufactured electrodes were electrochemically characterised against the near-ideal outer sphere redox probe $[Ru(NH_3)_6]^{3+}$ and inner-sphere probe $[Fe(CN)_6]^{4-}$, where it was seen that all bespoke additively manufactured electrodes significantly outperformed the commercial alternative. In particular, CO and TOTM plasticised filaments produced excellent results, with the PEG plasticiser producing good results and also exhibiting significant levels of increased baseline current. When applied to the electroanalytical detection of dopamine, CO and TOTM again produced excellent results along with the PEG additively manufactured electrode. The DOTP-plasticised electrode performed poorly in terms of the linear range and exhibited a significant anodic shift in the peak potential, most likely due to enhanced adsorption of dopamine on the additively manufactured electrode surface. The best overall performance of additively manufactured electrodes was observed for the filaments plasticised with CO, TOTM and PEG.

Data availability

The data supporting this article have been included in the main paper and as part of the ESI.†

Conflicts of interest

The authors declare no conflict of interest.

Acknowledgements

The authors would like to thank Dr Hayley Andrews for collecting SEM data. We thank EPSRC for funding (EP/W033224/1).

References

1 A. Standard, *ASTM International F2792-12a*, 2012, pp. 1–9.
2 M. J. Whittingham, R. D. Crapnell, E. J. Rothwell, N. J. Hurst and C. E. Banks, *Talanta Open*, 2021, **4**, 100051.
3 K. Ghosh and M. Pumera, *Nanoscale*, 2021, **13**, 5744–5756.
4 K. Ghosh and M. Pumera, *Small Methods*, 2021, **5**, 2100451.
5 B. Huener, N. Demir and M. F. Kaya, *Int. J. Hydrogen Energy*, 2022, **47**, 12136–12146.
6 C. Iffelsberger, S. Ng and M. Pumera, *Appl. Mater. Today*, 2020, **20**, 100654.
7 H. M. Elbardisy, E. M. Richter, R. D. Crapnell, M. P. Down, P. G. Gough, T. S. Belal, W. Talaat, H. G. Daabees and C. E. Banks, *Anal. Methods*, 2020, **12**, 2152–2165.
8 R. D. Crapnell, E. Bernalte, A. G.-M. Ferrari, M. J. Whittingham, R. J. Williams, N. J. Hurst and C. E. Banks, *ACS Meas. Sci. Au*, 2021, **2**, 167–176.
9 B. C. Janegitz, R. D. Crapnell, P. R. de Oliveira, C. Kalinke, M. J. Whittingham, A. G. M. Ferrari and C. E. Banks, *ACS Meas. Sci. Au*, 2023, **3**(3), 217–225.
10 J. Muñoz and M. Pumera, *ChemElectroChem*, 2020, **7**, 3404–3413.
11 C. Kalinke, P. R. De Oliveira, C. E. Banks, B. C. Janegitz and J. A. Bonacin, *Sens. Actuators, B*, 2023, **381**, 133353.
12 C. Kalinke, P. R. de Oliveira, B. C. Janegitz and J. A. Bonacin, *Sens. Actuators, B*, 2022, **362**, 131797.
13 C. Kalinke, N. V. Neumsteir, P. R. de Oliveira, B. C. Janegitz and J. A. Bonacin, *Anal. Chim. Acta*, 2021, **1142**, 135–142.
14 J. Muñoz and M. Pumera, *TrAC, Trends Anal. Chem.*, 2020, **128**, 115933.
15 C. Kalinke, N. V. Neumsteir, G. de Oliveira Aparecido, T. V. de Barros Ferraz, P. L. Dos Santos, B. C. Janegitz and J. A. Bonacin, *Analyst*, 2020, **145**, 1207–1218.
16 A. G.-M. Ferrari, N. J. Hurst, E. Bernalte, R. D. Crapnell, M. J. Whittingham, D. A. Brownson and C. E. Banks, *Analyst*, 2022, **147**, 5121–5129.
17 C. Iffelsberger, C. W. Jellett and M. Pumera, *Small*, 2021, **17**, 2101233.
18 R. G. Rocha, D. L. Ramos, L. V. de Faria, R. L. Germscheidt, D. P. dos Santos, J. A. Bonacin, R. A. Munoz and E. M. Richter, *J. Electroanal. Chem.*, 2022, **925**, 116910.
19 R. S. Shergill, C. L. Miller and B. A. Patel, *Sci. Rep.*, 2023, **13**, 339.
20 E. Vaněčková, M. Bouša, V. Shestivska, J. Kubišta, P. Moreno-García, P. Broekmann, M. Rahaman, M. Zlámal, J. Heyda, M. Bernauer, T. Sebechlebská and V. Kolivoška, *ChemElectroChem*, 2021, **8**, 2137–2149.
21 R. D. Crapnell, A. G. M. Ferrari, M. J. Whittingham, E. Sigley, N. J. Hurst, E. M. Keefe and C. E. Banks, *Sensors*, 2022, **22**, 9521.
22 R. D. Crapnell, C. Kalinke, L. R. G. Silva, J. S. Stefano, R. J. Williams, R. A. A. Munoz, J. A. Bonacin, B. C. Janegitz and C. E. Banks, *Mater. Today*, 2023, **71**, 73–90.
23 A. Godwin, *Applied plastics engineering handbook*, 2017.
24 K. Ghosh, S. Ng, C. Iffelsberger and M. Pumera, *Appl. Mater. Today*, 2022, **26**, 101301.
25 P. Wuamprakhon, R. D. Crapnell, E. Sigley, N. J. Hurst, R. J. Williams, M. Sawangphruk, E. M. Keefe and C. E. Banks, *Adv. Sustainable Syst.*, 2023, **7**, 2200407.
26 E. Sigley, C. Kalinke, R. D. Crapnell, M. J. Whittingham, R. J. Williams, E. M. Keefe, B. C. Janegitz, J. A. Bonacin and C. E. Banks, *ACS Sustainable Chem. Eng.*, 2023, **11**, 2978–2988.
27 I. V. Arantes, R. D. Crapnell, M. J. Whittingham, E. Sigley, T. R. Paixão and C. E. Banks, *ACS Appl. Eng. Mater.*, 2023, **1**, 2397–2406.
28 R. D. Crapnell, I. V. Arantes, M. J. Whittingham, E. Sigley, C. Kalinke, B. C. Janegitz, J. A. Bonacin, T. R. Paixão and C. E. Banks, *Green Chem.*, 2023, **25**, 5591–5600.
29 I. V. Arantes, R. D. Crapnell, E. Bernalte, M. J. Whittingham, T. R. Paixão and C. E. Banks, *Anal. Chem.*, 2023, **95**, 15086–15093.
30 R. D. Crapnell, I. V. Arantes, J. R. Camargo, E. Bernalte, M. J. Whittingham, B. C. Janegitz, T. R. Paixão and C. E. Banks, *Microchim. Acta*, 2024, **191**, 96.
31 C. Kalinke, R. D. Crapnell, E. Sigley, M. J. Whittingham, P. R. de Oliveira, L. C. Brazaca, B. C. Janegitz, J. A. Bonacin and C. E. Banks, *Chem. Eng. J.*, 2023, **467**, 143513.
32 E. M. Richter, D. P. Rocha, R. M. Cardoso, E. M. Keefe, C. W. Foster, R. A. Munoz and C. E. Banks, *Anal. Chem.*, 2019, **91**, 12844–12851.
33 J.-F. Veyan, E. de Obaldia, J. J. Alcantar-Peña, J. Montes-Gutierrez, M. J. Arellano-Jimenez, M. José Yacaman and O. Auciello, *Carbon*, 2018, **134**, 29–36.
34 X. Chen, W. Xiaohui and D. Fang, *Fullerenes, Nanotubes Carbon Nanostruct.*, 2020, **28**, 1048–1058.
35 T. R. Gengenbach, G. H. Major, M. R. Linford and C. D. Easton, *J. Vac. Sci. Technol., A*, 2021, **39**, 013204.
36 A. Fujimoto, Y. Yamada, M. Koinuma and S. Sato, *Anal. Chem.*, 2016, **88**, 6110–6114.
37 R. Blume, D. Rosenthal, J. P. Tessonnier, H. Li, A. Knop-Gericke and R. Schlögl, *ChemCatChem*, 2015, **7**, 2871–2881.
38 T. R. Gengenbach, G. H. Major, M. R. Linford and C. D. Easton, *J. Vac. Sci. Technol., A*, 2021, **39**, 013204.
39 R. D. Crapnell and C. E. Banks, *Talanta Open*, 2021, **4**, 100065.

40 W. B. Veloso, T. R. L. C. Paixão and G. N. Meloni, *Electrochim. Acta*, 2023, **449**, 142166.
41 X. Ji, C. E. Banks, A. Crossley and R. G. Compton, *ChemPhysChem*, 2006, **7**, 1337–1344.
42 H. T. Ahmed, V. J. Jalal, D. A. Tahir, A. H. Mohamad and O. G. Abdullah, *Results Phys.*, 2019, **15**, 102735.
43 D. L. Swinya, D. Martín-Yerga, M. Walker and P. R. Unwin, *J. Phys. Chem. C*, 2022, **126**, 13399–13408.